Equivalent loads for two-dimensional distributed anisotropic piezoelectric transducers with arbitrary shapes attached to thin plate structures

Arnaud Deraemaeker[a] and Gilles Tondreau
Université Libre de Bruxelles-BATir, 50 av. F.D. Roosevelt, CP 194/02 B-1050 Brussels

Frédéric Bourgeois
Department of Mathematics, Université Libre de Bruxelles, Boulevard du Triomphe, CP 218 B-1050 Brussels

(Received 28 April 2010; revised 1 October 2010; accepted 8 November 2010)

When a voltage is applied across the electrodes of a flat piezoelectric transducer attached to a thin plate structure, the transducer acts as equivalent loads applied to the host plate structure. In this paper, analytical expressions of these equivalent loads are derived for the general case of an orthotropic piezoelectric actuator using Hamilton's principle and two different mathematical approaches leading to the same results: Green's theorem and derivation using the theory of distributions. The equivalent loads are a function of the material properties as well as the normal to the contour of the transducer. Examples of applications to simple geometric shapes (triangle, rectangle, and circle) are given.
 [DOI: 10.1121/1.3523338]

PACS number(s): 43.38.Fx, 43.40.Dx, 43.40.Vn, 43.40.Yq [AZ] Pages: 1–10

I. INTRODUCTION

Piezoelectric transducers are commonly used in active vibration control and structural health monitoring applications. In particular, thin piezoelectric sensors and actuators are used to induce bending vibrations or propagating waves in plate-like structures. The main advantages of such transducers are their small size, their broad bandwidth, and their relatively low price. The most common piezoelectric flat transducers are made either of lead zircanium titanium (PZT) ceramic material (for actuation and/or sensing) or of polymer polyvinylidene fluoride (PVDF) material (mainly for sensing). During the last ten years, composite piezoelectric transducers have appeared on the market. By mixing piezoelectric fibers with a softer epoxy matrix, the composite transducers are more flexible and more robust[1] and exhibit orthotropic properties. Typical piezoelectric transducers found on the market are rectangular or circular. Different researchers have however studied the possibility to use more complex shapes. This idea was mainly driven by the active control applications. The first developments in this direction concern triangular actuators.[2] Using the theory of distributions and the beam theory, the authors show that applying a voltage difference V across the electrodes of the transducer is equivalent to applying two point forces and one bending moment on the supporting structure (Fig. 1). If the triangular actuator is clamped along one edge, the resulting force is a single point force at the tip of the triangle. Coupling this transducer with an accelerometer placed at the tip of the triangle leads to a collocated actuator/sensor pair and the possibility to develop a simple and theoretically stable control strategy.[3] Shaped transducers have also been used for the design of modal sensors and actuators,[4] as an alternative to modal filters obtained from discrete sensor arrays suffering from the spatial aliasing effect and more recently in order to measure the bending moment at the boundary of structures.[5]

In Refs. 2, 4, and 5, the equivalent loads have been computed using the beam theory. In practice however, the effects in the direction transverse to the beam neutral axis cannot be neglected, as clearly demonstrated both numerically and experimentally in Ref. 6 for modal filters. In order to correctly compute the equivalent loads of thin piezoelectric transducers, it is therefore necessary to use the plate theory. For triangular actuators, equivalent loads have been computed using Kirchoff's plate theory and the theory of distributions in Refs. 7 and 8 using the general approach developed in Refs. 9 and 10. These equivalent loads are represented in Fig. 2. The figure shows that the equivalent loads consist in three point forces at the tips of the triangle and distributed lineic bending moments M_1 and M_2 along the edges. With such equivalent loads, the use of an actuator/sensor pair consisting of a triangular piezoelectric actuator and an accelerometer will not lead to a collocated pair anymore, therefore reducing the bandwidth of stability of the controller, as shown in Ref. 3. The results demonstrated in Ref. 7 using the theory of distributions in two dimensions are however surprising: Consider an isotropic piezoelectric material ($e_{31} = e_{32}$) and an equilateral triangle: The equivalent loads computed clearly violate the symmetries of the problem. We conclude that the equivalent loads of Fig. 2 are not correct. This fact has also been noticed very recently in Ref. 11. At the same period, equivalent loads were derived for piezoelectric transducers with different shapes in Ref. 12. The study was limited to isotropic piezoelectric materials, and equivalent loads for a rhombus shape showed the appearance of point forces. Here again, if the rhombus is made of two equilateral triangles, the symmetries of the problem are violated, showing that the equivalent loads are not correct. Note that the results for rectangular actuators presented in Refs. 7

F1 F2

[a]Author to whom correspondence should be addressed. Electronic mail: Arnaud.Deraemaeker@ulb.ac.be

 0001-4966/2011/129(1)/1/10/$30.00

ID: mohanambigaid Time: 17:04 I Path: Q:/3b2/JAS#/Vol00000/100149/APPFile/AI-JAS#100149

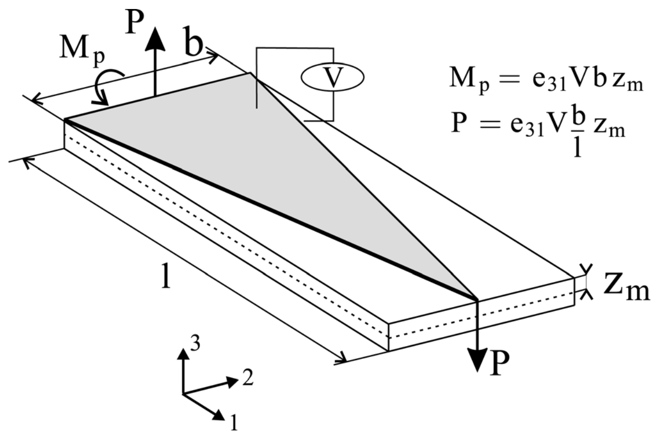

FIG. 1. Equivalent loads of a triangular piezoelectric transducer computed using Euler–Bernoulli beam theory.

and 9 are correct, because the edges of the patch are aligned with the structural axes. In fact, the main difficulty for the computation of the equivalent loads arises when the edges are not aligned with the structural axes, such as in the case of the triangular actuator or the rhombus.

The motivation of this study is to derive the correct analytical expressions of the equivalent loads for orthotropic piezoelectric actuators with arbitrary shapes, with the only limitation that the contour must be a piecewise smooth curve. These analytical expressions are derived based on Hamilton's principle using the flux linkage formulation for piezoelectric structures and two different mathematical approaches: (i) Green's theorem and (ii) the theory of distributions in two dimensions. The results show that the equivalent loads are a function of the material properties as well as the analytical expression of the normal to the contour. Finally, as an illustration, we give the equivalent loads for triangular, rectangular, and circular transducers in the case of orthotropic and isotropic piezoelectric materials. The application to a triangular transducer leads to equivalent loads which are different from the ones found in Ref. 7 and do not violate the symmetries for an equilateral triangle with isotropic piezoelectric material. In particular, we show that for an isotropic piezoelectric triangular actuator, there exist only lineic moments along the edges and no point forces.

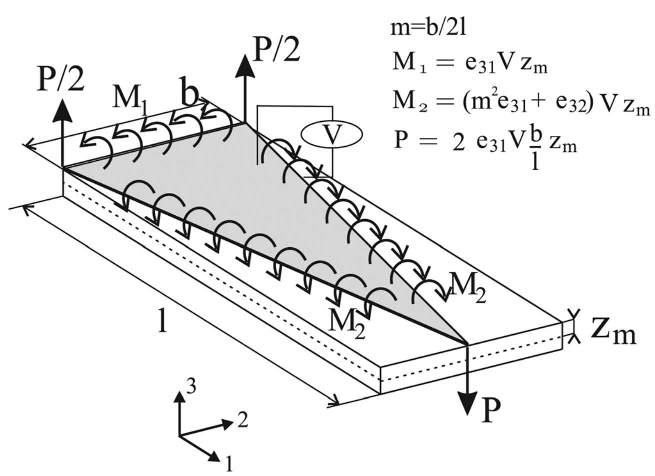

FIG. 2. Equivalent loads of a triangular piezoelectric transducer computed using Kirchoff's plate theory, from Ref. 7.

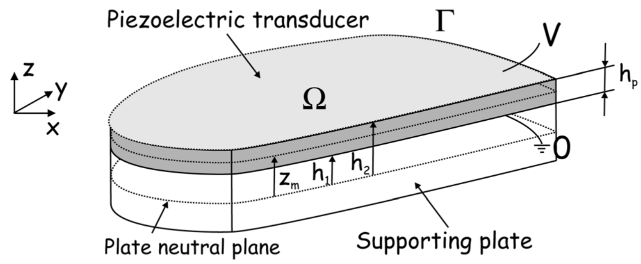

FIG. 3. Two-dimensional piezoelectric transducer attached on a plate.

II. NOTATIONS

Consider a two-dimensional piezoelectric transducer of thickness h_p attached on a plate along a plane region Ω (Fig. 3). We denote by Γ the closed curve bounding this region Ω. We assume that there is no prescribed displacement on this boundary. Let x, y be cartesian coordinates along the neutral plane of the plate, parallel to the plane containing Ω, and let z be the normal coordinate, so that $h_1 \le z \le h_2$ in the transducer with $h_p = h_2 - h_1$ and $z = 0$ is the neutral plane of the supporting plate. We denote by $z_m = \frac{1}{2}(h_1 + h_2)$ the distance between the mid-plane of the transducer and the neutral plane of the supporting plate.

In these coordinates, the displacement field will be denoted by $(u, v, w)^T$. Using Kirchoff's thin plate theory, the displacements are approximated by

$$\begin{aligned} u(x,y,z) &= u_0(x,y,0) - z w_{,x}, \\ v(x,y,z) &= v_0(x,y,0) - z w_{,y}, \\ w(x,y,z) &= w(x,y). \end{aligned} \tag{1}$$

The poling direction of the piezoelectric transducer is assumed to be in direction z and according to the plane stress hypothesis, the out of plane stress components are equal to zero. A voltage difference V is applied between the top and bottom surface electrodes of the transducer, resulting in an electric field $E_3 = -V/h_p$ in the z-direction ($E_1 = E_2 = 0$).

Using the standard Institute of Electrical and Electronics Engineers (IEEE) notations for linear piezoelectricity, the constitutive equations (under the plane stress hypothesis and in the material axes) for the transducer are given by

$$\begin{pmatrix} T_1 \\ T_2 \\ T_6 \\ D_3 \end{pmatrix} = \begin{pmatrix} c_{11}^E & c_{12}^E & 0 & -e_{31} \\ c_{21}^E & c_{22}^E & 0 & -e_{32} \\ 0 & 0 & c_{66}^E & 0 \\ e_{31} & e_{32} & 0 & \varepsilon_{33}^S \end{pmatrix} \begin{pmatrix} S_1 \\ S_2 \\ S_6 \\ E_3 \end{pmatrix},$$

where E_i and D_i are the components of the electric field vector and the electric displacement vector, respectively, and T_i and S_i are the components of stress and strain vectors, respectively, defined according to

$$\begin{Bmatrix} T_1 \\ T_2 \\ T_6 \end{Bmatrix} = \begin{Bmatrix} T_{11} \\ T_{22} \\ T_{12} \end{Bmatrix} \qquad \begin{Bmatrix} S_1 \\ S_2 \\ S_6 \end{Bmatrix} = \begin{Bmatrix} S_{11} \\ S_{22} \\ 2S_{12} \end{Bmatrix}.$$

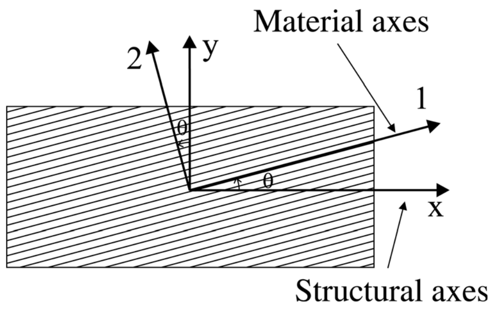

FIG. 4. Orientation of the material axes $1, 2$ with respect to the structural axes x, y.

The constitutive equations can also be written in a matrix form

$$\{T\} = \left[c^E\right]\{S\} - [e]\{E\},$$

and

$$\{D\} = [e]^T\{S\} + \left[\varepsilon^S\right]\{E\}. \tag{2}$$

Assume that the piezoelectric transducer's material axes make an angle θ with the structural axes noted x, y (Fig. 4). In this case, the stress vector is expressed in the structural axes as

$$\{T\}_{xy} = [R_T]^{-1}\left[c^E\right][R_S]\{S\}_{xy} - [R_T]^{-1}[e]\{E\}$$

and the electric displacement $\{D\}$ is given by

$$\{D\} = [e]^T[R_S]\{S\}_{xy} + \left[\varepsilon^S\right]\{E\},$$

with (see for example Ref. 13)

$$[R_T]^{-1} = \begin{bmatrix} \cos^2\theta & \sin^2\theta & -2\cos\theta\sin\theta \\ \sin^2\theta & \cos^2\theta & 2\cos\theta\sin\theta \\ \cos\theta\sin\theta & -\cos\theta\sin\theta & \cos^2\theta - \sin^2\theta \end{bmatrix}$$

and

$$[R_S] = \begin{bmatrix} \cos^2\theta & \sin^2\theta & \sin\theta\cos\theta \\ \sin^2\theta & \cos^2\theta & -\sin\theta\cos\theta \\ -2\sin\theta\cos\theta & 2\sin\theta\cos\theta & \cos^2\theta - \sin^2\theta \end{bmatrix}.$$

One can easily check that

$$[R_T]^{-1}[e] = \left([e]^T[R_S]\right)^T$$

so that the constitutive equations written in the structural axes can be written in the general form

$$\{T\}_{xy} = \left[c^{E*}\right]\{S\}_{xy} - [e^*]\{E\},$$

and

$$\{D\} = [e^*]^T\{S\}_{xy} - \left[\varepsilon^S\right]\{E\}.$$

Note that when matrix $[e^*]$ is expressed in the structural axes and angle $\theta \neq 0$, we have

$$[e^*] = \begin{bmatrix} e^*_{31} \\ e^*_{32} \\ e^*_{36} \end{bmatrix},$$

with

$$e^*_{31} = e_{31}\cos^2\theta + e_{32}\sin^2\theta,$$
$$e^*_{32} = e_{31}\sin^2\theta + e_{32}\cos^2\theta,$$
$$e^*_{36} = (e_{31} - e_{32})\cos\theta\sin\theta.$$

It is important to point out the fact that e^*_{36} is not a material parameter as such and is a function of e_{31}, e_{32}, and θ (for piezoelectric materials $e_{36} = 0$). Note also that for an isotropic piezoelectric material ($e_{31} = e_{32}$), we have $e^*_{36} = 0$.

The supporting plate is assumed to be purely elastic so that the constitutive equations (written in the structural axes) reduce to Hooke's law

$$\begin{pmatrix} T_1 \\ T_2 \\ T_6 \end{pmatrix} = \begin{pmatrix} c_{11} & c_{12} & 0 \\ c_{21} & c_{22} & 0 \\ 0 & 0 & c_{66} \end{pmatrix}\begin{pmatrix} S_1 \\ S_2 \\ S_6 \end{pmatrix}.$$

Using the small strain hypothesis, the strain components written in the structural axes are given by

$$S_1 = u_{,x}, \quad S_2 = v_{,y}, \quad \text{and} \quad S_6 = u_{,y} + v_{,x}. \tag{3}$$

III. HAMILTON'S PRINCIPLE USING THE FLUX LINKAGE FORMULATION APPLIED TO PIEZOELECTRIC STRUCTURES

In previous works, the equivalent loads resulting from the application of a voltage difference V between the electrodes of a piezoelectric patch attached to a plate (Fig. 3) were computed by applying the differential operator L on a spatial distribution $\Lambda(x, y)$[7,9]

$$L(\Lambda(x,y)) = -z_m V\left(e^*_{31}\frac{\partial^2\Lambda(x,y)}{\partial x^2} + e^*_{32}\frac{\partial^2\Lambda(x,y)}{\partial y^2} + 2e^*_{36}\frac{\partial^2\Lambda(x,y)}{\partial x\partial y}\right). \tag{4}$$

$\Lambda(x, y)$ has a unitary value inside the boundary of the piezoelectric patch and a zero value outside. Because of the discontinuity of $\Lambda(x, y)$ at the boundaries of the piezoelectric patch, the second derivatives must be computed using the theory of distributions. The derivatives involve Dirac distributions and their derivatives, and it is not always straightforward to interpret these functions in terms of equivalent loads, especially when the edges of the piezoelectric patch are not aligned with the structural axes. It seems that this is the origin of the erroneous computation of the equivalent loads for the triangle[7] and the rhombus[12] in previous works. In the following, we show that using Hamilton's principle the interpretation of the equivalent loads is straightforward.

The piezoelectric transducer is assumed to be thin compared to the thickness of the plate so that bending and in-plane motion are not coupled. In addition, in-plane motion is not considered so that only the equations related to the bending of the plate will be derived. In piezoelectric structures, the total change of energy density stored in a unit volume is given by the sum of the mechanical and the electrical work, expressed here in the material axes

$$dw_e(S,D) = \{dS\}^T\{T\} + \{dD\}^T\{E\}.$$

Differentiating $w_e(S,D)$ and comparing with the expression above leads to

$$\{T\} = \left\{\frac{\partial w_e}{\partial S}\right\} \qquad \{E\} = \left\{\frac{\partial w_e}{\partial D}\right\} \tag{5}$$

The coenergy density[14] is obtained through the Legendre transform

$$w_e^*(S,E) = \{E\}^T\{D\} - w_e(S,D),$$

and its differential is given by

$$dw_e^*(S,E) = \{dE\}^T\{D\} + \{E\}^T\{dD\} - \{dS\}^T\left\{\frac{\partial w_e}{\partial S}\right\} - \{dD\}^T\left\{\frac{\partial w_e}{\partial D}\right\},$$

which, using Eq. (5), reduces to

$$dw_e^*(S,E) = \{dE\}^T\{D\} - \{dS\}^T\{T\},$$

and using Eq. (2) we get

$$dw_e^*(S,E) = \{dE\}^T([e]^T\{S\} + [\varepsilon^S]\{E\}) - \{dS\}^T([c^E]\{S\} - [e]\{E\}),$$

which is the differential of

$$w_e^*(S,E) = \frac{1}{2}\{E\}^T[\varepsilon^S]\{E\} + \{S\}^T[e]\{E\} - \frac{1}{2}\{S\}^T[c^E]\{S\}.$$

The total coenergy W_e^* stored in a volume V is therefore given by

$$W_e^* = \int_V w_e^* dV$$

which, in the case of the structure considered in Fig. 3 reads

$$W_e^* = \frac{1}{2}\int_{-h_1}^{h_2} dz \int_\Omega (\{E\}^T[\varepsilon^S]\{E\} + 2\{S\}^T[e]\{E\} - \{S\}^T[c^E]\{S\})d\Omega.$$

The total coenergy is now written in the structural axes leading to

$$W_e^* = \frac{1}{2}\int_{-h_1}^{h_2} dz \int_\Omega (\{E\}^T[\varepsilon^S]\{E\} + 2\{S\}_{xy}^T[e^*]\{E\} - \{S\}_{xy}^T[c^{E*}]\{S\}_{xy})d\Omega.$$

It can be split into the contributions of the supporting plate (in which case there is no dielectric or piezoelectric part) and the piezoelectric patch

$$W_e^* = \frac{1}{2}\int_{-h_1}^{h_1} dz \int_\Omega -\{S\}_{xy}^T[c]\{S\}_{xy} d\Omega + \frac{1}{2}\int_{h_1}^{h_2} dz \int_\Omega (\{E\}^T[\varepsilon^S]\{E\} + 2\{S\}_{xy}^T[e^*]\{E\} - \{S\}_{xy}^T[c^{E*}]\{S\}_{xy})d\Omega.$$

Hamilton's principle using the flux linkage formulation (Ref. 14, p. 121) reads

$$\int_{t_1}^{t_2} [\delta(T^* + W_e^*) + \delta W_{nc}]dt = 0 \tag{6}$$

for any virtual vertical displacement δw complying with the kinematic constraints and satisfying $\delta w(t_1) = \delta w(t_2) = 0$. Note that $\delta E = 0$ since the electric field is imposed on the transducer and constant. T^* is the kinetic coenergy given by

$$T^* = \frac{1}{2}\int_{-h_1}^{h_2} dz \int_\Omega \rho \dot{w}^2 d\Omega.$$

Taking into account the fact that $\delta w(t_1) = \delta w(t_2) = 0$, we find

$$\int_{t_1}^{t_2} \delta T^* dt = -\int_{t_1}^{t_2} dt \int_\Omega (\rho h)_{eq} \ddot{w} \delta w d\Omega$$

with

$$(\rho h)_{eq} = 2h_1\rho_S + h_p\rho_p,$$

where ρ_S is the density of the supporting plate and ρ_p is the density of the piezoelectric material.

Equations (1) and (3) (Kirchhoff's plate theory) are used to derive the virtual strains

$$\delta S_1 = -z\delta w_{,xx}, \quad \delta S_2 = -z\delta w_{,yy}, \quad \text{and} \quad \delta S_6 = -2z\delta w_{,xy},$$

so that the variation of the coenergy function is given by

$$\delta W_e^* = -\int_\Omega (A(x,y)\delta w_{,xx} + B(x,y)\delta w_{,yy} + C(x,y)\delta w_{,xy})d\Omega, \tag{7}$$

with

$$A(x,y) = (Jc_{11})_{eq} w_{,xx} + (Jc_{12})_{eq} w_{,yy} - z_m e_{31}^* V,$$
$$B(x,y) = (Jc_{21})_{eq} w_{,xx} + (Jc_{22})_{eq} w_{,yy} - z_m e_{32}^* V,$$
$$C(x,y) = 4(Jc_{66})_{eq} w_{,xy} - 2z_m e_{36}^* V.$$

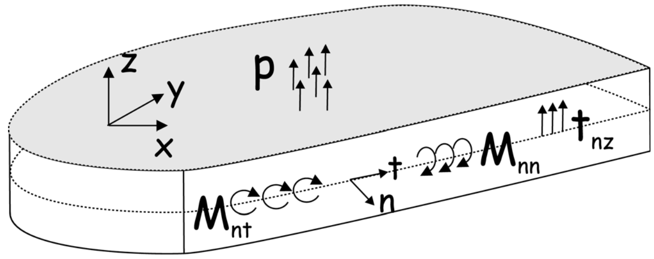

FIG. 5. Distributed external forces acting on the plate.

in which

$$(Jc_{ij})_{eq} = J_p c_{ij}^{E*} + J_s c_{ij} \quad \text{with} \quad J_p = \frac{h_2^3 - h_1^3}{3},$$
$$J_s = 2\frac{h_1^3}{3}.$$

$(Jc_{ij})_{eq}$ is the total bending stiffness equal to the sum of the bending stiffness of the supporting plate $J_s c_{ij}$ and of the piezoelectric patch $J_p c_{ij}^{E*}$. Note also that E_3 has been replaced by $-V/h_p$ in the computation. The virtual work of the external forces is given by

$$\delta W_{nc} = \int_\Omega p\delta w d\Omega + \int_\Gamma \left(-\frac{\partial M_{nt}}{\partial s} + t_{nz}\right)\delta w d\Gamma - \int_\Gamma M_{nn}\delta w_{,n} d\Gamma, \tag{8}$$

where p is the pressure acting on the plate, M_{nn}, M_{nt}, and t_{nz} are the distributed bending moment, torsional moment and shear forces acting on Γ (Fig. 5).

IV. COMPUTATION OF THE EQUIVALENT LOADS USING GREEN'S THEOREM

Reexpressing the integrand of Eq. (7) using Leibniz's law and applying Green's theorem, we obtain, after lengthy but straightforward computations,

$$\begin{aligned}\delta W_e^* = &-\int_\Omega (A_{,xx} + B_{,yy} + C_{,xy})\delta w d\Omega \\ &- \int_\Gamma (An_x^2 + Bn_y^2 + Cn_x n_y)\delta w_{,n} d\Gamma \\ &+ \int_\Gamma (A_{,x}n_x + B_{,y}n_y + C_{,x}n_y)\delta w d\Gamma \\ &+ \int_\Gamma \frac{\partial}{\partial s}((B-A)n_x n_y + Cn_x^2)\delta w d\Gamma.\end{aligned}$$

This formula is valid for a domain Ω bounded by a curve Γ of class C^1. Assume now that Γ is piecewise smooth and is obtained as the union of smooth curves Γ_i, $i = 1, \ldots, N$ starting at point p_{i-1} and ending at point p_i, with $p_N = p_0$. Then we can approximate Γ with a curve Γ_ϵ of class C^1 obtained by rounding the corners of Γ with arcs of circles of radii ϵ. We denote by Ω_ϵ the domain enclosed by Γ_ϵ. As ϵ tends to zero, the domain Ω_ϵ approaches Ω an the curve Γ_ϵ approaches Γ. Applying the above formula to Ω_ϵ and Γ_ϵ with $\epsilon \to 0$, we see that the first three integrals converge to identical expressions involving Ω and Γ because the integrands are bounded. However, the fourth integrand is not because n_x and n_y vary quickly over the small arcs of circles. The integral over the arc near p_i is equal to the variation of $(B-A)n_x n_y + Cn_x^2$ over this arc. Let us denote the discontinuity jump of a function g defined on Γ at point p_i by $[g]_i = g(p_i+) - g(p_i-)$. With this notation, as $\epsilon \to 0$, this variation converges to $(B-A)[n_x n_y]_i + C[n_x^2]_i$. Hence, in the case of a piecewise smooth curve Γ, the above formula becomes

$$\begin{aligned}\delta W_e^* = &-\int_\Omega (A_{,xx} + B_{,yy} + C_{,xy})\delta w d\Omega \\ &- \int_\Gamma (An_x^2 + Bn_y^2 + Cn_x n_y)\delta w_{,n} d\Gamma \\ &+ \int_\Gamma (A_{,x}n_x + B_{,y}n_y + C_{,x}n_y)\delta w d\Gamma \\ &+ \int_\Gamma \frac{\partial}{\partial s}((B-A)n_x n_y + Cn_x^2)\delta w d\Gamma \\ &+ \sum_{i=1}^N (B-A)[n_x n_y]_i + C[n_x^2]_i.\end{aligned}$$

Substituting $\delta W_e^*, \delta T^*$, and δW_{nc} in Eq. (6), we get the dynamic equation of motion in Ω

$$(A_{,xx} + B_{,yy} + C_{,xy}) + (\rho h)_{eq}\ddot{w} = p$$

and the two boundary conditions on Γ

$$\begin{aligned}(An_x^2 + Bn_y^2 + Cn_x n_y) &= -M_{nn}, \\ -\Bigg((A_{,x}n_x + B_{,y}n_y + C_{,x}n_y) &+ \frac{\partial}{\partial s}((B-A)n_x n_y + Cn_x^2) \\ &+ (B-A)[n_x n_y] + C[n_x^2]\Bigg) \\ &= -\frac{\partial M_{nt}}{\partial s} + t_{nz},\end{aligned}$$

where […] denotes the discontinuity jump at the considered point.

The piezoelectric contributions (terms in e_{ij}^*) in $A(x,y)$, $B(x,y)$, and $C(x,y)$ are independent of $w(x,y)$ so that they can be put in the right-hand side showing that applying a voltage difference V between the electrodes is equivalent to applying the following loads to the supporting plate:

$$\begin{aligned}-p &= \frac{\partial^2}{\partial x^2}(e_{31}^* z_m V) + \frac{\partial^2}{\partial y^2}(e_{32}^* z_m V) + 2\frac{\partial^2}{\partial x \partial y}(e_{36}^* z_m V), \\ -M_{nn} &= e_{31}^* n_x^2 z_m V + e_{32}^* n_y^2 z_m V + 2e_{36}^* n_x n_y z_m V, \\ -\left(-\frac{\partial M_{nt}}{\partial s} + t_{nz}\right) &= \frac{\partial}{\partial s}((e_{32}^* - e_{31}^*)n_x n_y z_m V + 2e_{36}^* n_x^2 z_m V) \\ &\quad + ((e_{32}^* - e_{31}^*)[n_x n_y] + 2e_{36}^*[n_x^2])z_m V \\ &\quad + \frac{\partial}{\partial x}(e_{31}^* z_m V)n_x + \frac{\partial}{\partial y}(e_{32}^* z_m V)n_y \\ &\quad + 2\frac{\partial}{\partial x}(e_{36}^* z_m V)n_y.\end{aligned} \tag{9}$$

In the most common case in which $e^*_{31}, e^*_{32}, e^*_{36}, z_m,$ and V are constant, the equivalent loads are

$$\begin{aligned}
&p = 0,\\
&M_{nn} = -e^*_{31} n_x^2 z_m V - e^*_{32} n_y^2 z_m V - 2e^*_{36} n_x n_y z_m V,\\
&-\frac{\partial M_{nt}}{\partial s} + t_{nz} = -(e^*_{32} - e^*_{31}) z_m V \frac{\partial}{\partial s}(n_x n_y) - 2e^*_{36} z_m V \frac{\partial}{\partial s}(n_x^2)\\
&\qquad\qquad - ((e^*_{32} - e^*_{31})[n_x n_y] + 2e^*_{36}[n_x^2]) z_m V,
\end{aligned}$$

and for isotropic piezoelectric material ($e_{31} = e_{32}$), we find

$$\begin{aligned}
&p = 0,\\
&M_{nn} = -e_{31} z_m V,\\
&-\frac{\partial M_{nt}}{\partial s} + t_{nz} = 0.
\end{aligned}$$

V. DERIVATION OF THE EQUIVALENT LOADS USING DISTRIBUTIONS IN TWO DIMENSIONS

A. Distributions in two dimensions

Consider the space of smooth functions φ with compact support (in other words, $\varphi = 0$ outside a large disk) in the plane with variables x and y. In this context, a distribution f associates, to every function φ, a scalar $\langle f, \varphi \rangle$ depending linearly and continuously (for a suitable topology) on φ.

For example, if $f(x, y)$ is a (locally integrable) function on the plane, then it defines a distribution, still denoted f, by

$$\langle f, \varphi \rangle = \int_{-\infty}^{+\infty} \int_{-\infty}^{+\infty} f(x, y)\varphi(x, y) dx dy.$$

The function $f(x, y)$ can be thought of as a density for the distribution f. Note however that some distributions are not defined through a density function.

In our computations, we shall use a couple of operations on distributions. First, for any distribution f and any smooth function ψ, the multiplication ψf is the distribution defined by

$$\langle \psi f, \varphi \rangle = \langle f, \psi \varphi \rangle.$$

Next, for any distribution f, its derivatives $f_{,x}$ and $f_{,y}$ are the distributions defined by

$$\langle f_{,x}, \varphi \rangle = -\langle f, \varphi_{,x} \rangle \quad \text{and} \quad \langle f_{,y}, \varphi \rangle = -\langle f, \varphi_{,y} \rangle.$$

This definition is inspired from integration by parts, in the case f is defined via a density function.

In the computation of the efforts for the transducer, we shall encounter the following four examples of distributions:

(1) Let Ω be a region of the plane. The characteristic distribution $\mathbb{1}_\Omega$ of Ω is defined by

$$\langle \mathbb{1}_\Omega, \varphi \rangle = \int_\Omega \varphi(x, y) d\Omega.$$

(2) Let Γ be a smooth curve in the plane, not necessarily closed. The Dirac distribution δ_Γ along Γ is defined by

$$\langle \delta_\Gamma, \varphi \rangle = \int_\Gamma \varphi(x, y) d\Gamma.$$

(3) Let n be the normal vector of the above curve Γ and g be a smooth function defined on Γ. Then the distribution $\frac{\partial}{\partial n}(g\delta_\Gamma)$ is given by

$$\left\langle \frac{\partial}{\partial n}(g\delta_\Gamma), \varphi \right\rangle = -\int_\Gamma g(x, y)\varphi_{,n}(x, y) d\Gamma.$$

(4) Let $p = (x_0, y_0)$ be a point of the plane. The Dirac distribution δ_p at point p is defined by

$$\langle \delta_p, \varphi \rangle = \varphi(x_0, y_0).$$

B. Computation of the efforts

The quantity δW_{nc} can be seen as the result of applying a distribution T_W to the function δw

$$\delta W_{nc} = \langle T_W, \delta w \rangle.$$

Moreover, Eq. (8) shows that this distribution decomposes in three terms, involving the first three examples of distributions in Sec. V A

$$T_W = p\mathbb{1}_\Omega + \left(-\frac{\partial M_{nt}}{\partial s} + t_{nz}\right)\delta_\Gamma + \frac{\partial}{\partial n}(M_{nn}\delta_\Gamma). \qquad (10)$$

On the other hand, we have shown in Sec. IV that the piezoelectric loads were given by the piezoelectric part in the expression of $-\delta W^*_e$, which, before applying Green's theorem, is given by

$$\begin{aligned}
-\delta W^*_e|_p &= \int_\Omega -z_m e^*_{31} V \delta w_{,xx} - z_m e^*_{32} V \delta w_{,yy}\\
&\quad - 2z_m e^*_{36} V \delta w_{,xy} d\Omega\\
&= \langle -z_m e^*_{31} V \mathbb{1}_\Omega, \delta w_{,xx} \rangle + \langle -z_m e^*_{32} V \mathbb{1}_\Omega, \delta w_{,yy} \rangle\\
&\quad + \langle -2z_m e^*_{36} V \mathbb{1}_\Omega, \delta w_{,xy} \rangle,
\end{aligned}$$

and using the definition of the derivatives of distributions, we get

$$\begin{aligned}
-\delta W^*_e|_p &= \left\langle -\frac{\partial^2}{\partial x^2}(z_m e^*_{31} V \mathbb{1}_\Omega), \delta w \right\rangle\\
&\quad + \left\langle -\frac{\partial^2}{\partial y^2}(z_m e^*_{32} V \mathbb{1}_\Omega), \delta w \right\rangle\\
&\quad + \left\langle -\frac{\partial^2}{\partial x \partial y}(2z_m e^*_{36} V \mathbb{1}_\Omega), \delta w \right\rangle.
\end{aligned}$$

We have therefore

$$\begin{aligned}
T_W &= -\frac{\partial^2}{\partial x^2}(z_m e^*_{31} V \mathbb{1}_\Omega) - \frac{\partial^2}{\partial y^2}(z_m e^*_{32} V \mathbb{1}_\Omega)\\
&\quad - 2\frac{\partial^2}{\partial x \partial y}(z_m e^*_{36} V \mathbb{1}_\Omega).
\end{aligned}$$

We now have to compute the effect of the differential operator $L = \frac{\partial^2}{\partial x^2}(e_{31}^*\cdot) + \frac{\partial^2}{\partial y^2}(e_{32}^*\cdot) + 2\frac{\partial^2}{\partial x \partial y}(e_{36}^*\cdot)$ on $\mathbb{1}_\Omega$, as in Eq. (4) from Ref. 9 and to identify the result with Eq. (10) in order to interpret the results in the form of equivalent efforts.

This computation is a generalization of the computation in Ref. 15 Sec. II 2 3. The first derivatives of the distribution $\mathbb{1}_\Omega$ are given by

$$\frac{\partial}{\partial x}\mathbb{1}_\Omega = n_x \delta_\Gamma, \quad \text{and} \quad \frac{\partial}{\partial y}\mathbb{1}_\Omega = n_y \delta_\Gamma.$$

As in Sec. IV, let us consider the case of a piecewise smooth curve Γ. For this, we decompose Γ as the union of smooth curves Γ_i, $i = 1, \ldots, N$ starting at point p_{i-1} and ending at point p_i, with $p_N = p_0$. then $\delta_\Gamma = \sum_{i=1}^N \delta_{\Gamma_i}$.

Let us compute the first derivatives of $n_x \delta_{\Gamma_i}$ and $n_y \delta_{\Gamma_i}$.

$$\begin{aligned}\left\langle \frac{\partial}{\partial x}(n_x \delta_{\Gamma_i}), \varphi \right\rangle &= -\int_{\Gamma_i} n_x \frac{\partial}{\partial x}\varphi d\Gamma \\ &= -\int_{\Gamma_i} n_x^2 \frac{\partial}{\partial n}\varphi d\Gamma + \int_{\Gamma_i} n_x n_y \frac{\partial}{\partial s}\varphi d\Gamma \\ &= \left\langle \frac{\partial}{\partial n}(n_x^2 \delta_{\Gamma_i}), \varphi \right\rangle + \int_{\Gamma_i} \frac{\partial}{\partial s}(n_x n_y \varphi) d\Gamma \\ &\quad - \int_{\Gamma_i} \frac{\partial}{\partial s}(n_x n_y)\varphi d\Gamma \\ &= \left\langle \frac{\partial}{\partial n}(n_x^2 \delta_{\Gamma_i}), \varphi \right\rangle + \langle n_x^{\Gamma_i} n_y^{\Gamma_i}(\delta_{p_i} - \delta_{p_{i-1}}), \varphi \rangle \\ &\quad - \left\langle \frac{\partial}{\partial s}(n_x n_y)\delta_{\Gamma_i}, \varphi \right\rangle.\end{aligned}$$

Hence,

$$\frac{\partial}{\partial x}(n_x \delta_{\Gamma_i}) = \frac{\partial}{\partial n}(n_x^2 \delta_{\Gamma_i}) + n_x^{\Gamma_i} n_y^{\Gamma_i}(\delta_{p_i} - \delta_{p_{i-1}}) - \frac{\partial}{\partial s}(n_x n_y)\delta_{\Gamma_i},$$

and summing over i, we deduce

$$\frac{\partial}{\partial x}(n_x \delta_\Gamma) = \frac{\partial}{\partial n}(n_x^2 \delta_\Gamma) - \sum_{i=1}^N [n_x n_y]\delta_{p_i} - \frac{\partial}{\partial s}(n_x n_y)\delta_\Gamma,$$

where $[n_x n_y]$ denotes the discontinuity jump of $n_x n_y$ at the considered point. Similarly, we have

$$\begin{aligned}\frac{\partial}{\partial y}(n_x \delta_\Gamma) &= \frac{\partial}{\partial n}(n_x n_y \delta_\Gamma) + \sum_{i=1}^N [n_x^2]\delta_{p_i} + \frac{\partial}{\partial s}(n_x^2)\delta_\Gamma, \\ \frac{\partial}{\partial x}(n_y \delta_\Gamma) &= \frac{\partial}{\partial n}(n_x n_y \delta_\Gamma) - \sum_{i=1}^N [n_y^2]\delta_{p_i} - \frac{\partial}{\partial s}(n_y^2)\delta_\Gamma, \\ \frac{\partial}{\partial y}(n_y \delta_\Gamma) &= \frac{\partial}{\partial n}(n_y^2 \delta_\Gamma) + \sum_{i=1}^N [n_x n_y]\delta_{p_i} + \frac{\partial}{\partial s}(n_x n_y)\delta_\Gamma.\end{aligned}$$

In other words, the second derivatives of $\mathbb{1}_\Omega$ are

$$\begin{aligned}\frac{\partial^2}{\partial x^2}\mathbb{1}_\Omega &= \frac{\partial}{\partial n}(n_x^2 \delta_\Gamma) - \sum_{i=1}^N [n_x n_y]\delta_{p_i} - \frac{\partial}{\partial s}(n_x n_y)\delta_\Gamma, \\ \frac{\partial^2}{\partial y \partial x}\mathbb{1}_\Omega &= \frac{\partial}{\partial n}(n_x n_y \delta_\Gamma) + \sum_{i=1}^N [n_x^2]\delta_{p_i} + \frac{\partial}{\partial s}(n_x^2)\delta_\Gamma, \\ \frac{\partial^2}{\partial x \partial y}\mathbb{1}_\Omega &= \frac{\partial}{\partial n}(n_x n_y \delta_\Gamma) - \sum_{i=1}^N [n_y^2]\delta_{p_i} - \frac{\partial}{\partial s}(n_y^2)\delta_\Gamma, \\ \frac{\partial^2}{\partial y^2}\mathbb{1}_\Omega &= \frac{\partial}{\partial n}(n_y^2 \delta_\Gamma) + \sum_{i=1}^N [n_x n_y]\delta_{p_i} + \frac{\partial}{\partial s}(n_x n_y)\delta_\Gamma.\end{aligned}$$

Note that the second and third lines agree, since $n_x^2 + n_y^2 = 1$.

Combining these derivatives and those of $z_m V$ with the coefficients e_{31}^*, e_{32}^* and e_{36}^*, we obtain

$$\begin{aligned}L(z_m V \mathbb{1}_\Omega) = &\left[\frac{\partial^2}{\partial x^2}(z_m e_{31}^* V) + \frac{\partial^2}{\partial y^2}(z_m e_{32}^* V)\right. \\ &\left. + 2\frac{\partial^2}{\partial x \partial y}(z_m e_{36}^* V)\right]\mathbb{1}_\Omega \\ &+ \left[2\frac{\partial}{\partial x}(z_m e_{31}^* V)n_x + 2\frac{\partial}{\partial y}(z_m e_{32}^* V)n_y\right. \\ &\left. + 2\frac{\partial}{\partial x}(z_m e_{36}^* V)n_y + 2\frac{\partial}{\partial y}(z_m e_{36}^* V)n_x\right]\delta_\Gamma \\ &+ z_m V\left(e_{31}^*\frac{\partial}{\partial n}(n_x^2 \delta_\Gamma) + e_{32}^*\frac{\partial}{\partial n}(n_y^2 \delta_\Gamma)\right. \\ &\left. + 2e_{36}^*\frac{\partial}{\partial n}(n_x n_y \delta_\Gamma)\right) \\ &+ \sum_{i=1}^N ((e_{32}^* - e_{31}^*)[n_x n_y] + 2e_{36}^*[n_x^2])z_m V \delta_{p_i} \\ &+ \left((e_{32}^* - e_{31}^*)\frac{\partial}{\partial s}(n_x n_y) + 2e_{36}^*\frac{\partial}{\partial s}(n_x^2)\right)z_m V \delta_\Gamma.\end{aligned}$$

Substituting $\frac{\partial}{\partial x} = -n_y\frac{\partial}{\partial s} + n_x\frac{\partial}{\partial n}$ and $\frac{\partial}{\partial y} = n_x\frac{\partial}{\partial s} + n_y\frac{\partial}{\partial n}$ in some terms of the second bracket, then incorporating the resulting terms with $\frac{\partial}{\partial n}$ in the third bracket and the terms with $\frac{\partial}{\partial s}$ in the fifth bracket, we find

$$\begin{aligned}L(z_m V \mathbb{1}_\Omega) = &\left[\frac{\partial^2}{\partial x^2}(z_m e_{31}^* V) + \frac{\partial^2}{\partial y^2}(z_m e_{32}^* V)\right. \\ &\left. + 2\frac{\partial^2}{\partial x \partial y}(z_m e_{36}^* V)\right]\mathbb{1}_\Omega \\ &+ \left[\frac{\partial}{\partial x}(z_m e_{31}^* V)n_x + \frac{\partial}{\partial y}(z_m e_{32}^* V)n_y\right. \\ &\left. + 2\frac{\partial}{\partial x}(z_m e_{36}^* V)n_y\right]\delta_\Gamma \\ &+ \frac{\partial}{\partial n}((e_{31}^* n_x^2 + e_{32}^* n_y^2 + 2e_{36}^* n_x n_y)z_m V \delta_\Gamma) \\ &+ \sum_{i=1}^N ((e_{32}^* - e_{31}^*)[n_x n_y] + 2e_{36}^*[n_x^2])z_m V \delta_{p_i} \\ &+ \frac{\partial}{\partial s}(((e_{32}^* - e_{31}^*)n_x n_y + 2e_{36}^* n_x^2)z_m V)\delta_\Gamma. \quad (11)\end{aligned}$$

Comparing (10) and (11), we deduce the efforts for the transducer

$$
\begin{aligned}
-p &= \frac{\partial^2}{\partial x^2}(z_m e_{31}^* V) + \frac{\partial^2}{\partial y^2}(z_m e_{32}^* V) + 2\frac{\partial^2}{\partial x \partial y}(z_m e_{36}^* V),\\
-\left(-\frac{\partial M_{nt}}{\partial s} + t_{nz}\right) &= ((e_{32}^* - e_{31}^*)[n_x n_y] + 2e_{36}^*[n_x^2])z_m V\\
&\quad + \frac{\partial}{\partial s}(((e_{32}^* - e_{31}^*)n_x n_y + 2e_{36}^* n_x^2)z_m V)\\
&\quad + \frac{\partial}{\partial x}(z_m e_{31}^* V)n_x + \frac{\partial}{\partial y}(z_m e_{32}^* V)n_y\\
&\quad + 2\frac{\partial}{\partial x}(z_m e_{36}^* V)n_y\\
-M_{nn} &= (e_{31}^* n_x^2 + e_{32}^* n_y^2 + 2e_{36}^* n_x n_y)z_m V.
\end{aligned}
$$

In the second equation, the discontinuity jump vanishes everywhere, except at points $p_1, \ldots, p_N$. In other words, this can be interpreted as point forces at the points p_i.

This result is identical to Eq. (9) derived using Green's theorem. The main advantage of the use of the theory of distributions is to avoid the lengthy computations when using Green's theorem (not detailed in Sec. IV). In both cases, Hamilton's principle is used to interpret the results in terms of equivalent loads.

VI. APPLICATIONS

A. Triangular actuator

Let us consider the case when $e_{36}^* = 0$ (the material axes are aligned with the structural axes) and Ω is a triangle, so that $N = 3$ and n is piecewise constant, we have

$$
\begin{aligned}
-\frac{\partial M_{nt}}{\partial s} + t_{nz} &= -(e_{32} - e_{31})[n_x n_y]z_m V,\\
M_{nn} &= (-e_{31}n_x^2 - e_{32}n_y^2)z_m V.
\end{aligned}
$$

Placing the vertices of the triangle at points $p_1 = (0, -b/2)$, $p_2 = (l, 0)$, and $p_3 = (0, b/2)$ (Fig. 6), the normal vector is given by

$$
n = \begin{cases} (-1, 0) & \text{on the edge } p_1p_3,\\ \frac{1}{\sqrt{\frac{b^2}{4}+l^2}}\left(\frac{b}{2}, -l\right) & \text{on the edge } p_1p_2,\\ \frac{1}{\sqrt{\frac{b^2}{4}+l^2}}\left(\frac{b}{2}, l\right) & \text{on the edge } p_2p_3, \end{cases}
$$

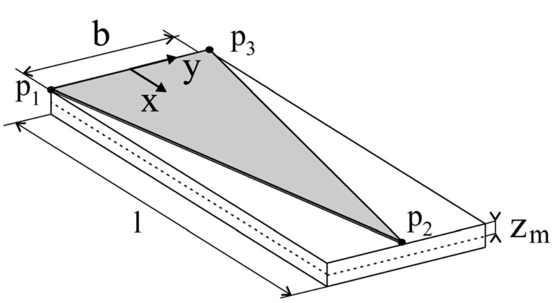

FIG. 6. Triangular actuator aligned with the structural axes.

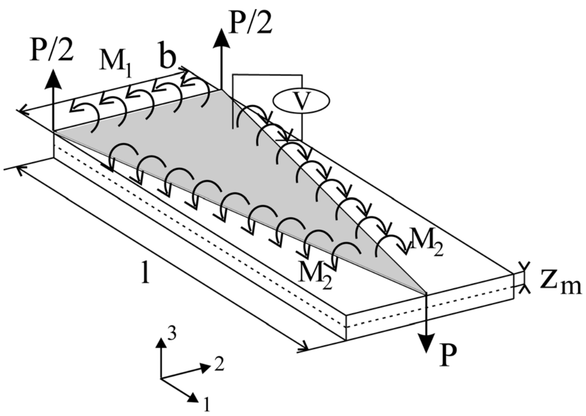

$$
\begin{aligned}
P &= -(e_{31} - e_{32})\frac{bl}{\frac{b^2}{4} + l^2}z_m V\\
M_1 &= -e_{31}z_m V\\
M_2 &= -\frac{\frac{b^2}{4}e_{31} + l^2 e_{32}}{\frac{b^2}{4} + l^2}z_m V
\end{aligned}
$$

FIG. 7. Equivalent loads for a triangular piezoelectric actuator.

so that

$$
-\frac{\partial M_{nt}}{\partial s} + t_{nz} = \begin{cases} (e_{32} - e_{31})\frac{bl}{2(\frac{b^2}{4}+l^2)}z_m V & \text{at point } p_1,\\ -(e_{32} - e_{31})\frac{bl}{\frac{b^2}{4}+l^2}z_m V & \text{at point } p_2,\\ (e_{32} - e_{31})\frac{bl}{2(\frac{b^2}{4}+l^2)}z_m V & \text{at point } p_3, \end{cases}
$$

$$
M_{nn} = \begin{cases} -e_{31}z_m V & \text{on the edge } p_1p_3,\\ -\frac{\frac{b^2}{4}e_{31}+l^2 e_{32}}{\frac{b^2}{4}+l^2}z_m V & \text{on the edge } p_1p_2,\\ -\frac{\frac{b^2}{4}e_{31}+l^2 e_{32}}{\frac{b^2}{4}+l^2}z_m V & \text{on the edge } p_2p_3. \end{cases}
$$

The equivalent loads are summarized in Fig. 7.

Note that for an isotropic triangle ($e_{31} = e_{32}$), there are no point forces and the distributed moments are $M_1 = M_2 = e_{31}z_m V$. This is in contradiction with the results previously derived in Refs. 7 and 12 which are not correct. This is easily shown, as stated before, by considering an isotropic equilateral triangle for which point forces of opposite sign cannot appear at the tips due to the symmetries of the problem. The general expressions derived in this paper show in fact that there are no point forces when $e_{31} = e_{32}$, whatever the shape of the contour.

B. Rectangular actuator with arbitrary orientation of the material axes

We consider the case when $e_{36}^* \neq 0$ (the material axes make an angle θ with the structural axes) and Ω is a rectangle, so that $N = 4$ and n is piecewise constant. On the whole contour Γ, the product $n_x n_y$ is equal to zero, leading to

$$
\begin{aligned}
-\frac{\partial M_{nt}}{\partial s} + t_{nz} &= -2e_{36}^*[n_x^2]z_m V,\\
M_{nn} &= -(e_{31}^* n_x^2 + e_{32}^* n_y^2)z_m V.
\end{aligned}
$$

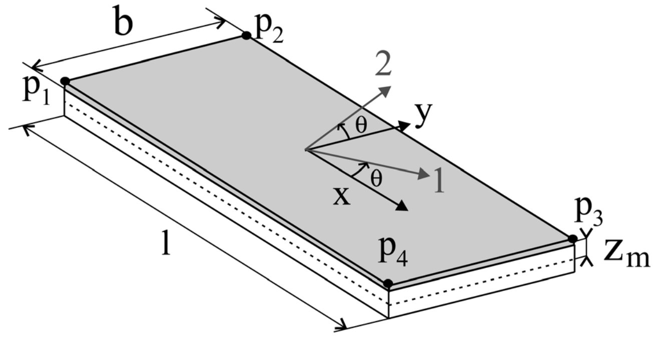

FIG. 8. Rectangular actuator with the material axes making an angle θ with the structural axes.

F8 Placing the vertices of the rectangle at points $p_1 = (0,0)$, $p_2 = (0,b)$, $p_3 = (l,b)$, and $p_4 = (l,0)$ (Fig. 8), the normal vector is given by

$$n = \begin{cases} (-1,0) & \text{on the edge } p_1p_2, \\ (0,1) & \text{on the edge } p_2p_3, \\ (1,0) & \text{on the edge } p_3p_4, \\ (0,-1) & \text{on the edge } p_4p_1 \end{cases}$$

so that

$$-\frac{\partial M_{nt}}{\partial s} + t_{nz} = \begin{cases} 2e^*_{36} z_m V & \text{at points } p_1 \text{ and } p_3, \\ -2e^*_{36} z_m V & \text{at points } p_2 \text{ and } p_4, \end{cases}$$

$$M_{nn} = \begin{cases} -e^*_{31} z_m V & \text{on the edges } p_1p_2 \text{ and } p_3p_4, \\ -e^*_{32} z_m V & \text{on the edges } p_2p_3 \text{ and } p_4p_1. \end{cases}$$

We recall that $e^*_{31}, e^*_{32}, e^*_{36}$ are a function of the material properties e_{31} and e_{32} and the orientation of the material axes with respect to the structural axes, given by the angle θ

$$e^*_{31} = e_{31}\cos^2\theta + e_{32}\sin^2\theta,$$
$$e^*_{32} = e_{31}\sin^2\theta + e_{32}\cos^2\theta,$$
$$e^*_{36} = (e_{31} - e_{32})\cos\theta\sin\theta.$$

F9 The equivalent loads are summarized in Fig. 9.

$$P = -2e^*_{36} z_m V$$
$$M_1 = -e^*_{31} z_m V$$
$$M_2 = -e^*_{32} z_m V$$

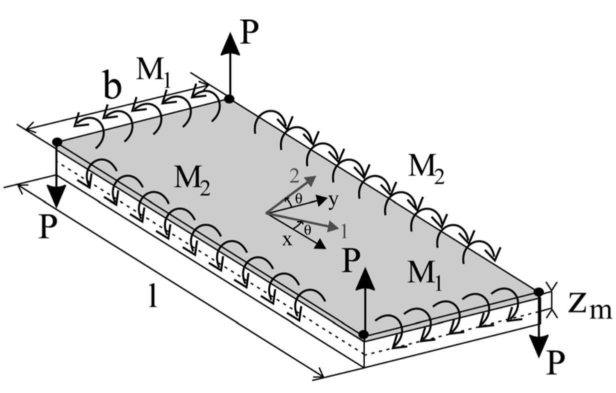

FIG. 9. Equivalent loads for a rectangular piezoelectric actuator.

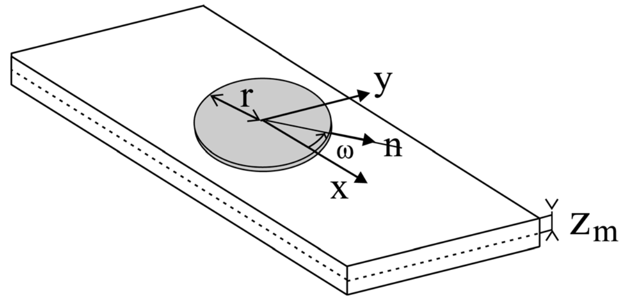

FIG. 10. Circular actuator with the reference angle given by the material axes.

Note again that for an isotropic rectangle ($e_{31} = e_{32}$), there are no point forces, and the distributed moments are $M_1 = M_2 = -e_{31} z_m V$. The results are in agreement with the ones published in Refs. 7 and 13.

C. Circular actuator

Without loss of generality, we will assume that the material axes are aligned with the structural axes, giving the reference angle for the expression of the equivalent loads (Fig. 10). We have $e_{36} = 0$ and $e^*_{31} = e_{31}$ and $e^*_{32} = e_{32}$, F10 $s = r\omega$ and the normal is a function of s given by

$$n_x = \cos\omega$$
$$n_y = \sin\omega$$

The equivalent loads are given by

$$-\frac{\partial M_{nt}}{\partial s} + t_{nz} = -\frac{\partial}{\partial s}\left((e_{32} - e_{31})\frac{\sin 2\omega}{2}\right) z_m V$$
$$= -\frac{1}{r}(e_{32} - e_{31})\cos 2\omega,$$
$$M_{nn} = -(e_{31}\cos^2\omega + e_{32}\sin^2\omega) z_m V.$$

In this case, because the normal depends on the position along the contour (defined by the angle ω), the generalized shear distribution $(-\frac{\partial M_{nt}}{\partial s} + t_{nz})$ and the normal bending moment M_{nn} are also angle dependant. Note that for an isotropic circular actuator ($e_{31} = e_{32}$), there is no generalized shear distribution on the contour, and the bending moment reduces to $M_{nn} = e_{31} z_m V$.

VII. CONCLUSION

Shaped piezoelectric transducers are used in a variety of applications. When a voltage difference is applied on the electrodes of such transducers, it results in a distribution of generalized loads applied to the host plate structure. In this paper, we have derived the analytical expressions of these equivalent loads assuming a piecewise linear contour. Hamilton's principle using the flux linkage formulation has been used and two different mathematical approaches have been used to derive the equivalent loads: Green's theorem and the theory of distributions in two dimensions. The main advantage of the theory of distributions is the simplicity of the calculations allowing to avoid the lengthy computations when

ID: mohanambigaid Time: 17:05 I Path: Q:/3b2/JAS#/Vol00000/100149/APPFile/AI-JAS#100149

using Green's theorem. Both approaches lead to the same analytical expressions of the equivalent loads which are a function of the topology of the contour (the normal of the contour and its discontinuities), the piezoelectric material properties, and the orientation of the material properties with respect to the structural axes. It is thought that such general expressions are presented for the first time in the literature. The equivalent loads have then been evaluated for triangular, rectangular, and circular orthotropic piezoelectric transducers in order to illustrate their application to simple geometric shapes. In particular, the results derived for the triangular actuator respect the symmetries for an isotropic equilateral triangle on the contrary to previously published results.

[1]A. Deraemaeker, H. Nasser, A. Benjeddou, and A. Preumont, "Mixing rules for the piezoelectric properties of Macro Fiber Composites," J. Intell. Mater. Syst. Struct. **20**(12), 1391–1518 (2009).

[2]S. E. Burke and J. E. Hubbard, "Active vibration control of a simply supported beam using a spatially distributed actuator," IEEE Control Syst. Mag. **7**(4), 25–30 (1987).

[3]P. Gardonio and S. J. Elliott, "Smart panels with velocity feedback control systems using triangularly shaped strain actuators," J. Acoust. Soc. Am. **117**, 2046–2064 (2005).

[4]C. K. Lee, W. W Chiang, and T. C. O'Sullivan, "Piezoelectric modal sensor/actuator pairs for critical active damping vibration control," J. Acoust. Soc. Am. **90**(1), 374–384 (1991).

[5]S. Chesne, B. Chomette, and C. Pezerat, "Measurements of the bending moment at boundaries of a structure," in *Proceedings of Acoustics08*, Paris, France (July 2008), pp. 1471–1476.

[6]A. Preumont, A. Francois, P. De Man, and V. Piefort, "Spatial filters in structural control," J. Sound Vib. **265**, 61–79 (2003).

[7]J. M. Sullivan, J. E. Jr., Hubbard, and S. E. Burke, "Modeling approach for two-dimensional distributed transducers of arbitrary spatial distribution," J. Acoust. Soc. Am. **99**, 2965–2974 (1996).

[8]J. M. Sullivan, Jr., J. E. Hubbard, and S. E. Burke, "Distributed sensor/actuator design for plates: Spatial shape and shading as design parameters," J. Sound Vib. **203**(3), 473–493 (1997).

[9]C. K. Lee and F. C. Moon, "Laminated piezopolymer plates for torsion and bending sensors and actuators," J. Acoust. Soc. Am. **85**(6), 2432–2439 (1989).

[10]C. K. Lee and F. C. Moon, "Modal sensors/actuators," J. Appl. Mech. **57**, 434–441 (1990).

[11]P. Gardonio, Y. Aoki, and S. J. Elliott, "A smart panel with active damping wedges along the perimeter," Smart Mater. Struct. **19**(6), 005003 (2010).

[12]V. Sonti, S. Kim, and J. Jones, "Equivalent forces and wavenumber spectra of shaped piezoelectric actuators," J. Sound Vib., **187**(1), 111–131 (1995).

[13]C. K. Lee, "Theory of laminated piezoelectric plates for the design of distributed sensors/actuators. Part I: Governing equations and reciprocal relationships," J. Acoust. Soc. Am. **87**(3), 1144–1158 (1990).

[14]A. Preumont, *Mechatronics: Dynamics of Electromechanical and Piezoelectric Systems* (Springer, Dordrecht, The Netherlands, 2006), pp. 1–207.

[15]L. Schwartz, *Méthodes mathématiques pour les sciences physiques (Mathematical methods for physical sciences), Collection enseignement des sciences 3, section II.2.3.* (Hermann, Paris, France, 1965).